A CARBON COMPOSITE DIVERGING VERTICAL TAIL FOR COMMERCIAL AIRPLANES

V. Venkayya and V. Tischler
Air Force Research Laboratory, U.S.
O. Sensburg, and T. Schweiger
Daimler Chrysler Aerospace, DE

Abstract

Carbon fiber vertical tails are not an unusual design feature for modern commercial airplanes. In this design study it is shown that with proper aeroelastic tailoring a vertical tail can achieve a directional stability derivative which is thirty percent higher than that of a rigid tail. Using this design feature the span and weight can be reduced accordingly

1. Introduction

In the past, design practice was to minimize elastic structural deflections to reduce undesirable aeroelastic phenomena. An opportunity for a paradigm shift has arisen in the design philosophy whereby these elastic deflections can be used to enhance the aerodynamic performance. Large weight savings, or performance improvements, can be expected by using the advantages of flexibility. In order to satisfy the other aeroelastic constraints (flutter, divergence, vibration response, etc.) it is necessary to approach the problem in a multidisciplinary manner. If Multidisciplinary Design Optimization (MDO) is not used, then an optimal design cannot be achieved due to the conflicting demands of the different disciplines.

The design of aircraft and space structures requires the marshalling of large teams of engineers to select the design that satisfies all the requirements. Typically this design goes through further refinement of modification, as more knowledge is gained about the requirements or as new conditions are imposed. Much of this effort consists presently of applying 'cut and try" procedures wherein the design is perturbed and reanalyzed many times. This redesign is required frequently, because two or more disciplines have conflicting demands that require compromise.

Vertical tails designed for high speed aircraft suffer from reduced stability and control effectiveness at high dynamic pressures due to aeroelastic effects. Therefore, adequate tail performance requires a large surface area with high aspect ratios and a stiff and heavy structure. These large surfaces are also subject to burst vortex or shock induced buffet that causes fatigue problems. Their size and structural constraints cause weight, drag, and radar-cross section penalties. These penalties can be significantly reduced by the application of aeroelastic optimization technologies to the vertical tail design problem, which results in a lighter structure and potentially smaller size to reduce buffet, drag and observability. In some cases the smaller size requirement could remove the necessity for multiple surfaces.

For high speed the vertical tail is designed to provide a certain minimum value of the directional static stability derivative. For low speed the rudder power must be adequate to hold a sideslip of $\beta=11.5^0$ at the approach speed for a cross wind landing. It also must cover the one engine out case. This low speed requirement may reduce the possibility to cut the fin span and area commensurate with positive high speed aeroelastics.

These requirements are the same for transport and fighter airplanes. Design load cases

are also equivalent and aspect ratios, taper ratios and sweep are very similar. Therefore, findings for combat aircraft are applicable to transport airplanes.

A Diverging Flexible Vertical Tail (DFVT) could be very useful for short fuselage versions if the static stability is a problem reducing the necessary span and weight. The reason why it is called 'diverging' is that a surface design with greater efficiency than 1.0 must diverge at some speed. Our aim must be that the divergence does not occur in the required speed range of the air vehicle.

The technology applied is called Active Flexible Technology which is a multidisciplinary, synergistic technology that integrates aerodynamics, controls, and structures together to maximize air vehicle performance shapes for optimum performance. This was first described extensively in [1] and [5].

If the low speed requirement is the design case, then an all moveable vertical tail could be the solution as is shown in this paper. An all moveable vertical tail is not a new invention. It was utilized on the very successful VSR71 Blackbird and on the VF117 stealth fighter. Also a British prototype aircraft of the 1960's, the TSR2, had a vertical tail. It was also considered seriously on the European fighter aircraft, EFA. Lately it was discussed in [2]. In the context of the DFVT it has several advantages:

- The rear yaw attachment can be moved far backward on the fin, because there is no rudder.
- It can also be utilized for the low speed regime (engine out or side wind requirement), where there is no aeroelastic effect, because the whole surface is rotated.

2. Description of Work

A generic aircraft design was selected, and the vertical tail was designed (at the conceptual design level) with conventional and with active flexible technologies. The weight, performance, and observables benefits of the DFVT were then determined relative to the conventional design. Figure 1 shows the comparison of a fighter vertical tail with the vertical tail of a future large transport aircraft.

A Finite Element Model (FEM) model was available which was used in the Dasa Lagrange optimization code [3]. This model was modified to serve for the USAF-ASTROS optimization code. The FEM could be very useful for future work as a benchmark. Therefore all comparison with the Dasa results are well documented.

Because of the low aspect ratio of the chosen vertical tail design, AR=1.2, this is an ideal candidate for applying aeroelastic tailoring for a carbon fiber composite structure (Fig. 2). As can be seen in the figure the higher the aspect ratio is, the higher are the weight penalties to meet the performance goals.

2.1 Formulation of the Design Study

A statement of the optimization problem for the design study is as follows:

Minimize or maximize:

$$F(\mathbf{X}) = F(X_1, X_2, \ldots, X_n) \qquad (1)$$

subject to a set of system response constraints

$$G_i (X_i, X_2, \ldots, X_n) \le G_{io} \quad i = 1,2,\ldots,p \qquad (2)$$

and constraints on the elements of the **X** vector

$$X^L \le X \le X^U \qquad (3)$$

The weight of the fin was selected as the objective function, F(**X**), for this study. The response constraints, G(**X**), were derived from the simultaneous analysis of the structure in three areas: a) static strength, b) static aeroelastic response and c) dynamic aeroelasticity - flutter. The variable vector, **X**, represents the thicknesses

and directional properties of the fiber reinforced composite skins.

The optimization problem was to find the optimal variable vector, **X**, that corresponds to the minimum weight of the structure without violating any of the response constraints defined by Equation (2). Also, this variable vector had to be within the range defined by Equation (3).

The solution of the optimization problem stated by Equations (1-3) involves three major steps:

1. Selection of an initial variable vector, $\mathbf{X}^0$
2. Evaluation of the objective and constraint functions, Equations (1-2)
3. A search strategy to move to a new variable vector, $\mathbf{X}^I$, in an n-dimensional design space, and eventually to the optimal vector, $\mathbf{X}_{opt}$.

This is an iterative procedure, and the issues of solution convergence need to be addressed. The first step, the selection of the initial vector, is generally arbitrary, although it will have a significant impact, if there is a potential for multiple minimums. The second step, objective and constraint function evaluation, is referred to as an analysis of the system, and it requires a significant computational effort for complex systems. Additional details of this step are discussed in the next subsection. The third step, the search strategy in n-dimensional space to locate the optimum point, depends on the type of algorithm selected. A first order optimization algorithm, also known as a gradient method, was used in the ASTROS software system in this study. Except for the zero-order methods, all other algorithms require an additional step called a sensitivity analysis. The ASTROS system uses analytical gradients based on the analysis used in the second step.

As stated previously, the function evaluations in the second step require an analysis, and in general, it is multidisciplinary, because of the type of response functions involved. In this study two types of aeroelastic response functions are addressed, in addition to the static strength of the structure:

- static aeroelasticiy
- dynamic aeroelasticity

A brief description of these two types of functions are given here. A more detailed discussion is given in References 4 and 6.

The response of a structure subjected to external forces can be described by a simple equation in the context of a finite element discretization of the structure, i.e.

$$\mathbf{KU} = \mathbf{P}(\mathbf{U}) \tag{4}$$

where **K** is the n x n stiffness matrix of the structure, and **U** is an nx1 vector of displacements, defined in reference to the structure's degrees of freedom. The left hand side of the equation represents the elastic forces in equilibrium with the aerodynamic forces on the right hand side. However, the forces due to the airflow are not independent of the deformation of the structure, and this is indicated by expressing **P** as a function of **U** as well. This is usually referred to as aeroelastic interaction. If the right hand side of the equation does not include inertia forces (accelerations are assumed to be zero), then it is referred to as static aeroelasticity.

An approximate form of **P(U)** can be written as

$$\mathbf{P}(\mathbf{U}) = q\mathbf{A}\mathbf{U} + q\mathbf{A}^{\alpha}\alpha + q\mathbf{A}^{\delta}\delta \tag{5}$$

where q is the dynamic pressure, $\frac{\rho V^2}{2}$, ρ is the air density and V is the free stream velocity. **A** is the aerodynamic influence coefficient matrix with respect to the displacement degrees of freedom. $\mathbf{A}^{\alpha}$ and $\mathbf{A}^{\delta}$ are due to the lifting surface and the control surface angles of attack. **α** is the initial angle of attack and **δ** is the control surface displacement.

The case of static divergence of the lifting surface is represented by

$$[\mathbf{K} - q\mathbf{A}]\mathbf{U} = 0 \qquad (6)$$

The solution of this complex eigenvalue problem (corresponding to the lowest real positive value) yields both the divergence dynamic pressure and the divergence velocity.

The lift effectiveness is another important static aeroelastic parameter, and it is defined as the ratio of the flexible lift to the rigid lift. It can be written as

$$\text{LE} = \frac{C_{LF}}{C_{LR}} = \frac{q\mathbf{h}^{\mathrm{T}}\mathbf{A}^{\alpha}\alpha + q\mathbf{h}^{\mathrm{T}}\mathbf{A}\mathbf{U}}{\mathbf{h}^{\mathrm{T}}\mathbf{A}^{\alpha}\alpha} \qquad (7)$$

where C_{LF} is the flexible lift curve slope and C_{LR} is its rigid counterpart, and where **h** is a vector consisting of the aerodynamic panel lengths. Solving Equation 5 for **U** with $\boldsymbol{\delta}$ = 0 and substituting into Equation 7 gives the lift effectiveness equation

$$\text{LE} = \frac{\mathbf{h}^{\mathrm{T}}\left[\mathbf{I} + q\mathbf{A}\left[\mathbf{K} - q\mathbf{A}\right]^{-1}\right]\mathbf{A}^{\alpha}\alpha}{\mathbf{h}^{\mathrm{T}}\mathbf{A}\alpha} \qquad (8)$$

Similar expressions can be derived for control surface effectiveness (aileron effectiveness) as well as flutter velocity constraints. They are implemented as constraints in the ASTROS system.

3. ASTROS Concepts

ASTROS was the computer code used for this study. ASTROS is a finite element based software system that has been designed to assist, to the maximum practical extent, in the preliminary design of aerospace structures. A concerted effort has been made to provide the user with a tool that has general capabilities with flexibility in their application.

A vital consideration in software of this type is that the key disciplines that impact the design must be included in the automated design task. This multidisciplinary aspect of the program has been implemented in an integrated way so that all the critical design conditions are considered simultaneously.

In addition to the interaction of several disciplines, ASTROS can treat multiple boundary conditions, and, within each boundary condition, multiple subcases. The system is not arbitrarily restricted by problem size, and it conforms to the current environment for performing structural analysis in the aerospace industry. The practical limitations on problem size are available disk space and data processing time.

Compatibility with the current aerospace environment is addressed, because the ASTROS procedures resemble those of NASTRAN in terms of user input and pre-and post-processor interfaces. While the ASTROS program doesn't contain many of the specialized capabilities available in NASTRAN, the basic structural analysis features have been included. Most importantly, from a user point-of-view, the Bulk Data formats have been taken directly from NASTRAN and modified only if the design considerations required such a modification in the data or, in a few cases, if minor changes result in superior capability. New Bulk Data entries have been created to input design information and data needed to run the steady aerodynamics and other analyses specific to ASTROS.

3.1 ASTROS Capabilities

This section gives a brief overview of the capabilities that are included in the code. The basic disciplines that are implemented within this code are as follows:

1. Static analysis
2. Modal and flutter analysis
3. Aerodynamic Analysis
4. Dynamic Response Analysis
5. Optimization

The static analysis methodology is based on a finite element representation of the structure, as are all the structural analysis disciplines in ASTROS. The static analysis module computes responses to statically applied mechanical (e.g.

discrete forces and moments), thermal and gravity loadings. Static deformations and their resultant stresses are among the computed responses. An extensive design capability is provided for the static analysis discipline. It provides the capability to analyze and design linear structures subjected to time invariant loading.

The modal analysis feature in ASTROS provides the capability to analyze and design linear structures for their modal characteristics, i.e. eigenvalues and eigenvectors. The design aspect of ASTROS places limits on the frequencies of the structure. The modal analysis is not only useful in its own right, but it also provides the basis for a number of further dynamics analyses. Flutter and blast response analyses in ASTROS are always performed in modal coordinates. Transient and frequency response analyses can be performed in either modal or physical coordinates, at the selection of the user.

Steady aerodynamics are used for the computation of external loads on aircraft structures. The static aeroelastic analysis features in ASTROS provide the capability to analyze and design linear structures in the presence of steady aerodynamic loading. This provides the ASTROS user with a self-contained capability to compute loads experienced by a maneuvering aircraft and to redesign the structure based on these loads. The capabilities available for steady aerodynamics design include specifying limits on (1) the allowable stress or strain response due to a specified trimmed maneuver, (2) the flexible to rigid ratio of the aircraft's lift curve slope, (3) the flexible roll control effectiveness of any antisymmetric control surface and (4) the values of the flexible stability derivatives and trim parameters.

Flutter analysis in ASTROS provides the capability to assess the aeroelastic stability characteristics of the designed structure and to correct any deficiencies in a systematic fashion. Both subsonic and supersonic analyses are available and reflecting the multidisciplinary character of the procedure, the design task can be performed with any number of boundary conditions and flight conditions. In this way, all critical flutter conditions can be analyzed and designed for simultaneously.

Dynamic analysis is performed for loadings which are a function of time or frequency.

The final discipline listed above is that of optimization. If only stress or strain constraints are included in the design task, the fully stressed design option may be used. For more general design tasks, a mathematical programming approach has been implemented. Details about the ASTROS code can be found in [4].

3.2 Structural Constraints for Vertical Tail Layout

- Strength or strain allowables must not be exceeded. Five load cases were used in this case.
- Static aeroelastic efficiencies for the vertical tail and the rudder were required. These are defined as flexible coefficients divided by the rigid coefficients.
- Flutter or divergence speed requirements, 530m/sec, Ma 1.2 for this case. For the transport aircraft it is reduced to 400 m/sec, Ma 0.9, which gives a relief, because static aeroleastic efficiency and flutter speed are conflicting targets.

In addition there are some specific composite requirements such as, minimum ply thickness and the maximum amount of one layer

4. Structural Description of the Fin and Rudder

The overall geometry of the fin is given in Figure 3. The surface area is 5.46 m^2 and the leading edge sweep angle is 45^0. The fin box has one shear pick-up in the front and one bending attachment at the rear. The rudder actuator is connected with two rods for control actuation. Fin box and rudder skins are built as carbon fiber laminates. A quasi isotropic glass fiber laminate is used for the tip structure with contains avionic

equipment. The fin box and rudder are coupled by three hinges.

These are the four materials which were used: Carbon Fiber Composite, CFC; Graphite Fiber Composite, GFC; Aluminum and Titanium.

1. Fin Box Skin - Four layer CFC laminate
2. Rudder Skin - Three layer CFC laminate
3. Tip Skin - Quasi Isotropic GFC
4. Fin Box Rear Spar - Four layer CFC laminate
5. Rudder Main Spar - Four layer CFC laminate
6. Remaining Spars - Aluminum
7. Fin Box End Rib - Titanium
8. Rudder End Ribs - Titanium
9. Remaining Ribs - Isotropic CFC

5. Comparison of NASTRAN and ASTROS Results with Existing Dasa Design

In order to become familiar with the Dasa finite element model of the fin and rudder several NASTRAN and ASTROS analyses were performed, and the results were compared with existing Dasa data. Correlation was found to be excellent. After that exercise the Dasa model was changed. To allow different attachment conditions the general stiffness element, GENEL, giving the effect of the fuselage stiffness, was removed and replaced with single attachment springs. These springs were tuned so that the model would give the original Dasa result. ASTROS and NASTRAN results are identical, because the ASTROS-code uses the finite element description of NASTRAN. The results of this comparison can be found in Table 1.

6. Results of the Optimization Runs with ASTROS

Several computer runs were performed with

- Strength Constraints
- Flutter speed 530/m/sec at Ma 1.2/S.L.
- Aeroelastic Efficiency

trying to match the Dasa results for a fin efficiency of 0.814 at Ma 1.8, 102 kPa. The rudder efficiency was fallout at 0.3799. The ASTROS code reduced the weight for this configuration to 81.1 kg. The weight of the initial design was 99.4 kg. When all the constraints were fulfilled, the weight was 95.1 kg for a fin efficiency of 0.814.

Higher fin efficiencies were requested, and the weights for these designs are plotted in Fig. 4. While 0.9 can be reached with very little extra weight, higher efficiencies need excessive weight penalties. When the rudder efficiency was treated as fallout, then the weight reduces considerably, and an efficiency of 1.0 can be reached when flutter is fallout too. The fallouts are quite reasonable and sufficient for a feasible design. From Fig. 4 it can be seen that a fin efficiency of 1.0 can only be achieved with infinite weight.

The picture changes completely when Ma 0.9 subsonic air forces are used (Fig. 5). Now efficiencies higher than 1.0 are reached. As can be seen, with very little additional weight, 1.3 can be reached for a high pressure of 102 kPa, which is not possible for air. The highest q is 57 kPa for Ma 0.9, i.e. sea level in air. This trend is also verified in Fig.6 which clearly shows that the wash-in angle increases for higher efficiencies, which simulates basically a forward swept fin behavior (diverging!).

7. Physical Explanation of the Basic Mechanism of the DFVT

In order to understand the elastic behavior of the fin, an equivalent beam is assumed which contains the stiffness of the fin. This beam would be located at the elastic axis, which is a spanwise line through the shear centers of each cross section. The shear center of each cross section is computed by establishing the point in the plane of the section at which a shear force can be applied without twisting the section or where a twisting moment can be applied to the section without producing a deflection at the shear center. An

effective elastic axis was defined by using the deflection of two points fore and aft on the chord, where a moment was applied at the tip, assuming small angles and that the deflection varies linearly along the chord. Fig. 7 shows the elastic axis location. From this figure one can assess why it is impossible to get a wash-in effect (diverging) for the supersonic Ma 1.8 case. The center of pressure – at 30% span and 50% chord – just reduces any initial angle of attack of the fin, and therefore the best fin efficiency which can be reached with aeroelastic tailoring is 1.0, which is the rigid behavior and needs a lot of structural weight. At the subsonic case, Ma 0.9, there exists some possibilities for wash-in, because the aeroelastic tailoring also shifts the so called elastic axis. This behavior is shown in Fig. 5 and also in Fig. 8 for an optimized case of Ma 0.9, 102 kPa and fin efficiency of 1.3.

8. Results for Shifting the Fin Attachments Back

This behavior changes drastically when the fin attachments are shifted back. The x-position for the forward attachment was shifted back from x = 450mm to x = 950 mm. The x-position for the rear attachment was shifted from x = 1750 mm to x =2300 mm. The new positions can be seen in Fig. 9. Now the centers of pressure are forward of the elastic axis, and wash-in behavior can be expected for both the subsonic and the supersonic cases (Fig. 9). For Ma 0.9, 57 kPa a fin efficiency of 1.3 can be reached with practically no weight increase. Also the rudder efficiency increases from 0.5 to 0.7. This can be seen in Figure 10. For the supersonic case Ma 1.8, 102kPa the behavior is similar (Fig. 11), and 1.3 can also be reached with an optimized laminate. The rudder efficiency is now reduced to 0.5. The flutter speed is 530m/sec. As an item of interest an analysis was performed (no optimization) to find the fin and rudder efficiency at Ma 0.9, 57kPa for the laminate of Ma 1.8, 102 kPa. This shows a fin efficiency of 1.3 and a rudder efficiency of 0.8. Figure 12 shows the thicknesses of Layer 1 and 8 for the fin box and the rudder skin for Ma 1.8, 102kPa and an effectiveness of 1.3.

9. Structural Representation of the All Moveable Vertical Tail

The rudder was attached with stiff rods to the fin. The forward attachment was reduced to a very low stiffness. Reducing this stiffness results in a low yaw stiffness, which in turn reduces the flutter speed considerably (Table 2).

9.1 Optimization Results

When the optimization code is used, a fin efficiency of 1.65 with a slightly reduced flutter speed of 500 m/sec can be achieved, which gives a 23% flutter margin at Ma 1.2 at sea level which is sufficient. Higher than 1.65 efficiency cannot be achieved (Fig. 13). For the subsonic case a fin efficiency of 3.04 is possible with a high enough flutter speed of 400 m/sec and a weight of 70.6 kg. The V-g plot for this case depicts a flutter and divergence speed at the same point.

10. Conclusions and Recommendations

A list of possible benefits is presented below:

- The reduced tail size reduces the CD_0 drag.

- The reduced span and area reduces the exposure to upstream induced burst vortex and separated flow unsteady pressure fields which increases tail buffet fatigue life. The increase in life reduces repair and replacement life cycle costs.

- The reduced planform size reduces observable signatures to increase stealth mission capability and reduce detectability.

- Because of the possible size reduction one vertical tail should be sufficient even for Navy airplanes.

- With proper multidisciplinary optimization a carbon fiber vertical tail can be made 30% more efficient that a rigid surface at the same weight.

- If the low speed requirement is not relevant, the area of the vertical tail can be reduced by 30% together with the structural weight.

- An all moveable vertical tail could be the optimum solution for a subsonic transport aircraft, because moving the whole tail would fulfill the low speed requirement.

- A wind tunnel model should be built and tested to prove the concept experimentally. An analytical method to lay out and fabricate a low cost wind tunnel model is available.

References

[1] Shirk, M. H., Hertz, T. J., and Weisshaar, T. A., A Survey of Aeroelastic Tailoring Theory, Practice, Promise ,*AIAA Paper AIAA-84-0982-CP*, *25th Structures, Structural Dynamics and Materials Conference*, Palm Springs, California, 1984

[2] Schweiger, D. and Krammer, J., Active Aeroelastic Aircraft and its Impact on Structure and Flight Control System Design, *AVT Panel Meeting Proceedings*, Ottawa, Canada, Fall 1999

[3] Schneider, G., Krammer, J., and Hornlein, H.R.E.M., First Approach to an Integrated Fin Design, *AGARD Report 784, Integrated Design Analysis and Optimization of Aircraft Structures*

[4] Neill, D.J., Herendeen, D.L., and Venkayya, V.B., *ASTROS Theoretical Manual*, USAF WL-TR-95-3006

[5] Pendleton, E., Bessette, D., Field, P., Miller, G., and Griffin, K., The Active Aeroelastic Wing Flight Research Program, *39th AIAA/ASME/ASCE/AHS/ASC Structures , Structural Dynamics, and Materials Conference*, April 1998

[6] Bowman, K.B., Grandhi, R.V., and Eastep, F.E., Structural Optimization of Lifting Surfaces with Divergence and Control Reversal Constraints, *Structural Optimization 1*, pgs 153-161, Springer-Verlag 1989

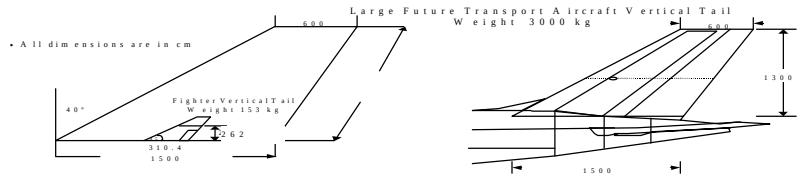

Fig 1 Comparison of a fighter vertical tail with the vertical tail of a future large transport aircraft

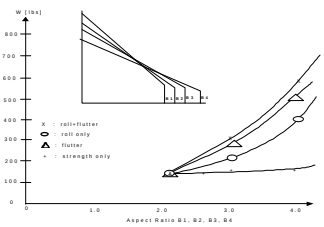

Fig 2 Structural weight for various constraints vs aspect ratio

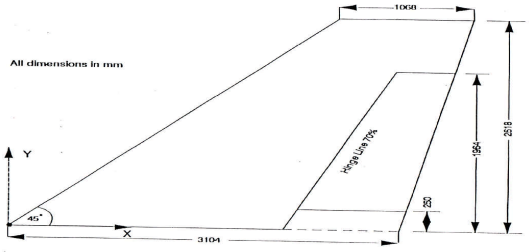

Fig 3 Fin Geometry

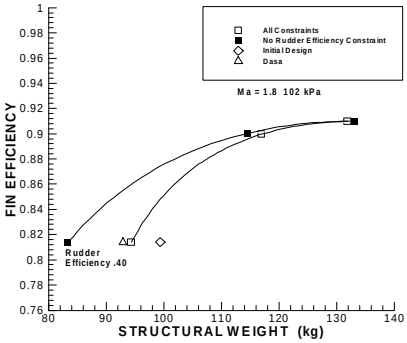

Fig 4 Fin efficiency vs structural weight Ma 1.8 102kPa

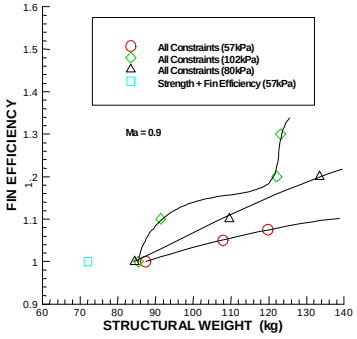

Fig 5 Fin efficiency vs structural weight Ma 0.9

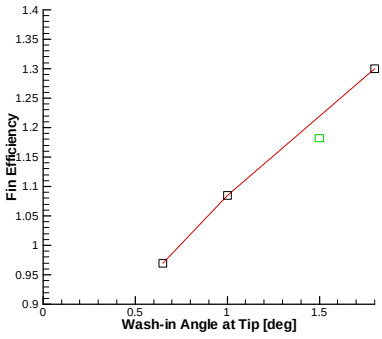

Fig 6 Fin efficiency vs wash-in angle at the tip

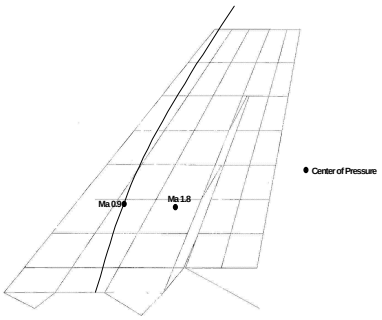

Fig 7 Elastic axis location (original attachments and DASA skin thicknesses)

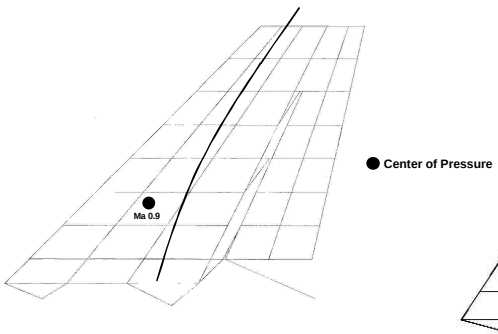

Fig 8 Elastic axis location for Ma 0.9 102kPa fin efficiency 1.3

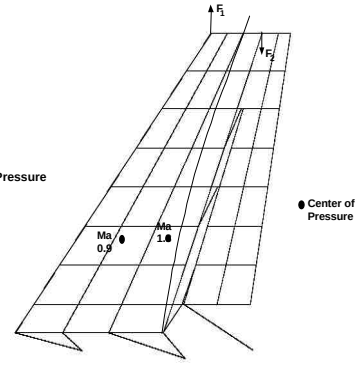

Fig 9 Elastic axis location (rear attachments)

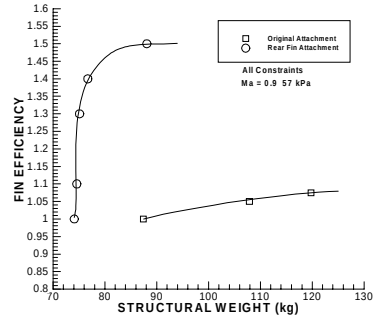

Fig 10 Fin efficiency vs structural weight Ma 0.0 57 kPa

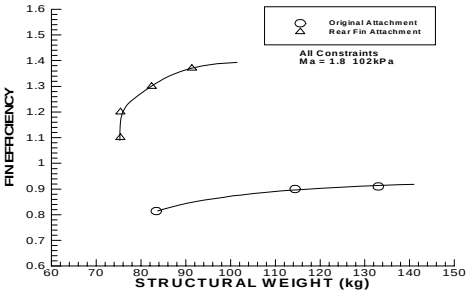

Figure 11 Fin efficiency vs structural weight Ma 1.8 102 kPa

	Initial Design ASTROS	Initial Design DASA	With Single Springs	Optimum Design	
				ASTROS	DASA
Weight [kg]					
Structure	99.4	99.4	99.4	94.3	92.9
Non Structure	53.6	53.6	53.6	53.6	53.6
Total	153.0	153.0	153.0	147.9	146.5
Deflections [mm]					
Load Case 1	304	291			
Load Case 2	384	367			
Load Case 3	148	154			
Load Case 4	220	231			
Load Case 5	146	159			
Frequencies [Hz]					
f_1	9.1	8.9	9.0	8.89	9.2
f_2	30.5	29.8	30.0	28.84 (f+a)	30.2 (f+a)
f_3	32.5(fore+aft)	31.2 (f+a)	43.9 (f+a)	41.03	30.6
f_4	41.4	40.0	41.6	42.39	41.08
f_5	55.7	54.9	57.6	59.36	58.31
Ma 1.2 S.L.					
Flutter Frequency – f_f [Hz}	20.2	21.2	20.0		
Speed –v_f [m/s]	493.4	495.0	534.0	530.0	530.0
Ma 1.8 102kPa –Aeroelastics					
Fin		0.753	0.740	0.814	0.814
Rudder		0.441	0.423	0.500	0.500
Aeroelastic Deflections [mm]					
Fin 1^0	65.34	53.7			
Rudder 1^0	8.88	8.29			

Table 1 Comparison of DASA and ASTROS results

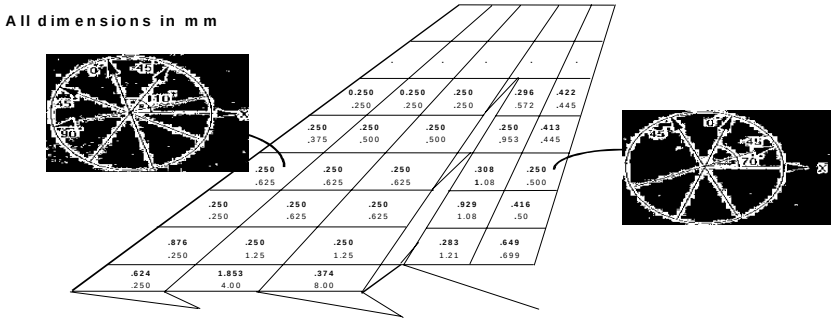

Fig 12 Thickness of layer 1 after optimization
(Ma 1.8 102 kPa 1.3 efficiency)

	Original DASA Sizes With Forward Attachment	Original DASA Sizes With Low Stiffness Forward Attachment
Mode 1	8.31 Hz	8.20 Hz
Mode 2	26.72 Hz	19.69 Hz
Mode 3	43.01 Hz (fore and aft)	43.01 Hz (fore and aft)
Mode 4	46.11 Hz	36.88 Hz
Mode 5	53.71 Hz	52.40 Hz
	Flutter Speed m/sec 526.00 Flutter Frequency Hz 18.27	375.04 13.95

Table 2 Influence of the forward attachment on the dynamic properties

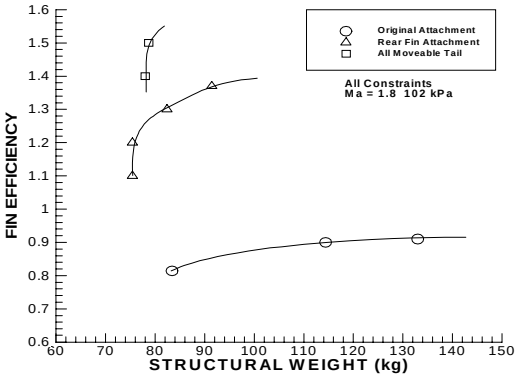

Figure 13 Fin efficiency vs structural weight for Ma 1.8 102 kPa